PHYSICAL REVIEW B VOLUME 27, NUMBER 4 15 FEBRUARY 1983

Photoluminescence spectra of the layered semiconductor gallium selenide under intense picosecond laser-pulse excitations

S. S. Yao and R. R. Alfano
Ultrafast Spectroscopy and Laser Laboratory, Physics Department, City College of New York, New York, New York 10031
(Received 22 March 1982)

The photoluminescence spectra of gallium selenide consist of two bands at both 77 and 300 K. The lower-energy part of the spectra is associated with stimulated emission. The higher-energy part of the spectra is assigned to the exciton-electron (-hole) scattering process at lower excitation intensity and to the electron-hole plasma at higher excitation intensity. From the analysis of the high-energy tails of the higher-energy part of the emission spectra, the transition from the exciton-carrier scattering emission to the electron-hole plasma emission at 300 K was obtained for an excitation intensity of about $(1.70\pm0.25)\times10^8$ W cm^{-2}.

I. INTRODUCTION

A layered semiconductor having interesting optical and electrical properties is gallium selenide (GaSe). From the measurements of the Hall mobility of the holes and the direct energy gap, Schmid[1] concluded that holes interact strongly with the homopolar optical phonons $A_1'^{(1)}$ ($=16.7$ meV). There is still uncertainty in the literature over the location of the fundamental energy gap of GaSe since the direct and indirect energy gaps are close to each other—within 10 meV.[2,3] The direct exciton absorption and emission were observed over a wide range of temperatures and attributed to the resonance effect[4] between the direct exciton state and the indirect conduction band.

Over the years many studies have been performed on the photoluminescence spectra of GaSe. Nahory *et al.*[5] reported the measurements of stimulated emission in single-crystal ϵ-GaSe, and showed that the emission arises from recombination across a direct band gap. Ugumori *et al.*[6,7] investigated the emission spectra from GaSe under nitrogen-laser excitation at 4.2 and 77 K. They observed two emission bands ascribed to the recombination of the exciton-electron and exciton-exciton collision processes. Mercier *et al.*[8] observed four lines at high excitations, of which two were attributed to exciton-carrier scattering: one arising from spontaneous emission and the other from stimulated emission. The two other lines correspond to two different exciton-exciton scattering processes. The stimulated emission was observed by Kuroda *et al.*,[9] who attributed the emission mechanism to the Auger process between the direct and the indirect excitons. The electron-hole plasma emission was observed on the lower-energy side of the exciton emission at both 77 and 300 K by Baltramiejunas *et al.*[10] using the second harmonic of a neodymium:glass laser. However, they did not observe the exciton-carrier scattering emission. The electron-hole plasma emission was also observed at the low-energy side of the stimulated emission line (S line) in the temperature range 77–300 K by Cingolani *et al.*[11] using a nitrogen pulsed laser. This result is different from our experimental result which shows that the electron-hole plasma emission is on the high-energy side of the S line when the sample temperature is at 300 K.

In this paper we have extended the above work and have measured the photoluminescence spectra from GaSe under high-power picosecond laser-pulse excitations at 77 and 300 K. Two emission bands were observed. The lower-energy band is attributed to stimulated emission and the higher-energy band arises from the exciton-electron (-hole) scattering at low excitation intensity $(0.7-1.6)\times10^8$ W cm^{-2} and the plasma effect at high intensity $(1.7-7)\times10^8$ W cm^{-2}. The transition from the exciton-carrier scattering emission to the electron-hole plasma emission was apparent from the spectral changes of band shape and emission maxima when the excitation was increased above 1.7×10^8 W cm^{-2}. The exciton-electron (-hole) scattering

emission changes into the plasma emission with the band gap reduced at room temperature as the excitation intensity was increased beyond 1.7×10^{8} W cm^{-2} (photogenerated carrier density $\sim3\times10^{17}$ cm^{-3}).

II. EXPERIMENTAL METHODS

A single 6-ps pulse at 0.53 μm from a Nd:glass laser was used to excite the GaSe sample on the front surface. The excitation area was 7 mm^2. The luminescence spectra emitted from the front surface was detected and analyzed using a $\frac{1}{4}$-m Spex spectrometer, a PAR SIT camera, and an optical multichannel analyzer (OMA). The polarization of the excitation pulse was perpendicular to the c axis which is normal to the layer of GaSe.

III. EXPERIMENTAL RESULTS

Two series of time-integrated photoluminescence from GaSe at different excitation intensities are shown in Figs. 1 and 2 at 77 and 300 K, respectively. As the excitation increases, the emission line shape changes at both temperatures.

In Fig. 1 as the intensity is increased from 10^{7} W cm^{-2} to 5×10^{8} W cm^{-2}, the two bands change. In Fig. 1(a), the excitation is $(0.15\pm0.02)\times10^{8}$ W cm^{-2}, two peak energies are 2.094 eV (5918 Å) and $\sim$2.049 eV (6050 Å); in Fig. 1(b), the excitation is $(0.21\pm0.03)\times10^{8}$ W cm^{-2}, two peak energies are 2.093 eV (5922 Å) and 2.048 eV (6048 Å); in Fig. 1(c), the excitation is $(0.22\pm0.03)\times10^{8}$ W cm^{-2}, two peak energies are 2.093 eV (5922 Å) and 2.051 eV (6044 Å), the intensity of the lower-energy band increases faster than that of the higher-energy band; in Fig. 1(d), the excitation is $(0.76\pm0.11)\times10^{8}$ W cm^{-2}, the higher-energy band cannot be observed clearly since the lower-energy band is so large, the peak energy is at 2.041 eV (6071 Å); and in Fig. 1(e), the excitation is $(5.07\pm0.74)\times10^{8}$ W cm^{-2} and the lower-energy emission peak is 2.024 eV (6124 Å).

Figure 2 shows that, as the intensity is increased, the two bands change. In Fig. 2(a), the excitation is $(0.82\pm0.12)\times10^{8}$ W cm^{-2}, the higher-energy peak is at 1.994 eV (6216 Å); in Fig. 2(b), the excitation intensity is $(0.97\pm0.14)\times10^{8}$ W cm^{-2}, the higher-energy peak is at 1.996 eV (6209 Å), the lower-energy band peak is not clear; in Fig. 2(c), the excitation intensity is $(1.34\pm0.20)\times10^{8}$ W cm^{-2}, the higher-energy peak is at 1.993 eV (6218 Å); in Fig.

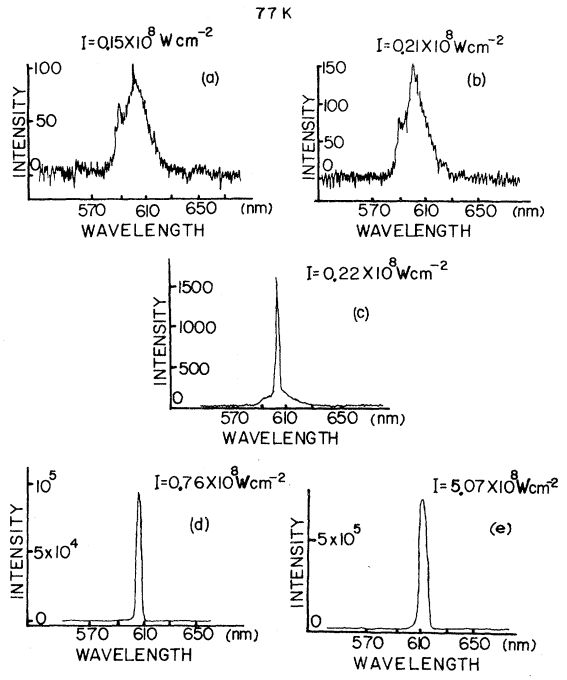

FIG. 1. Series of the photoluminescence spectra from GaSe at different 530-nm psec-pulse excitation intensities at 77 K. The excitation intensities (measured in units of 10^{8} W cm^{-2}) are as follows: (a) (0.15±0.02), (b) (0.21±0.03), (c) (0.22±0.03), (d) (0.76±0.11), and (e) (5.07±0.74).

2(d), the excitation intensity is $(1.61\pm0.24)\times10^{8}$ W cm^{-2}, the higher-energy peak is at 1.987 eV (6237 Å); in Fig. 2(e), the excitation intensity is $(1.70\pm0.25)\times10^{8}$ W cm^{-2}, the higher-energy peak is at 1.973 eV (6282 Å) which is smaller than that of Fig. 2(d); in Fig. 2(f), the excitation intensity is $(1.93\pm0.28)\times10^{8}$ W cm^{-2}, the higher-energy peak is at 1.973 eV (6282 Å) which is equal to that of Fig. 2(e); in Fig. 2(g), the excitation intensity is $(3.13\pm0.46)\times10^{8}$ W cm^{-2}, the higher-energy peak is at 1.964 eV (6311 Å) which is smaller than that of Fig. 2(f); in Fig. 2(h), the excitation intensity is $(3.86\pm0.56)\times10^{8}$ W cm^{-2}, the two peak energies are 1.962 eV (6318 Å) and 1.912 eV (6481 Å), the lower-energy-band intensity has increased faster than the higher-energy band which has smaller peak energy than that of Fig. 2(g); in Fig. 2(i), the excitation is $(4.15\pm0.61)\times10^{8}$ W cm^{-2}, the higher-energy-band intensity is very small compared with that of the lower-energy band which is peaked at 1.909 eV (6493 Å); and in Fig. 2(j), the excitation is $(7.1\pm1.0)\times10^{8}$ W cm^{-2}, the higher-energy band is not clearly recognizable but its intensity is still larger than that of Fig. 2(i), the lower-energy band

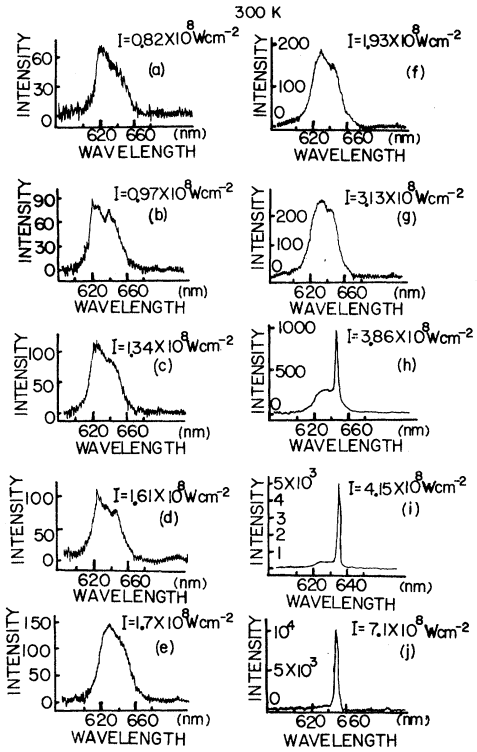

FIG. 2. Series of the photoluminescence spectra from GaSe at different 530-nm psec-pulse excitation intensities at room temperature. The excitation intensities (measured in units of 10^8 W cm^{-2}) are as follows: (a) (0.82±0.11), (b) (0.97±0.14), (c) (1.34±0.20), (d) (1.61±0.24), (e) (1.70±0.25), (f) (1.93±0.28), (g) (3.13±0.46), (h) (3.86±0.56), (i) (4.15±0.61), and (j) (7.1±1.0).

is peaked at 1.906 eV (6503 Å).

The emission intensity as a function of the excitation intensity is plotted in Figs. 3 and 4 for the observed two bands at 77 and 300 K, respectively.

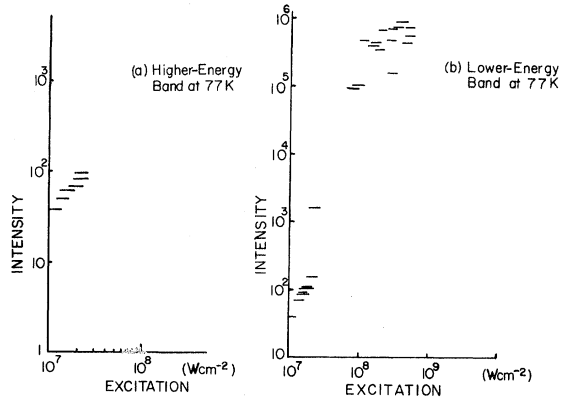

FIG 3. Emission intensity as a function of the 530-nm psec-pulse excitation intensity at 77 K. (a) Higher-energy band. (b) Lower-energy band.

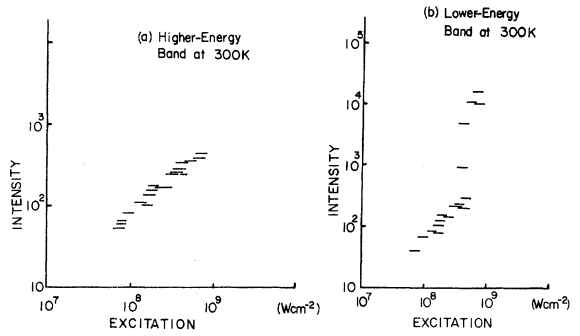

FIG. 4. Emission intensity as a function of the 530-nm psec-pulse excitation intensity at room temperature. (a) Higher-energy band. (b) Lower-energy band.

The intensity dependences for higher and lower band data at 77 K are displayed in Figs. 3(a) and 3(b), respectively. For the higher-energy band, the luminescence increases linearly with the excitation intensity. Beyond 2.5×10^7 W cm^{-2}, the higher-energy band is small as compared with the lower-energy band. The luminescence intensity dependence of the lower-energy band increases sharply with the excitation intensity. The luminescence intensity dependence on the excitation intensity for the higher- and lower-energy bands at 300 K are plotted in Figs. 4(a) and 4(b), respectively. The luminescence of the higher-energy band increases linearly with the excitation intensity. Above 4×10^8 W cm^{-2}, the higher-energy band is no longer apparent as compared with the lower-energy band which increases sharply with the excitation intensity from 3×10^8 to 8×10^8 W cm^{-2}.

The peaks of higher- and lower-energy luminescence bands are plotted in Fig. 5 for 300 and 77 K

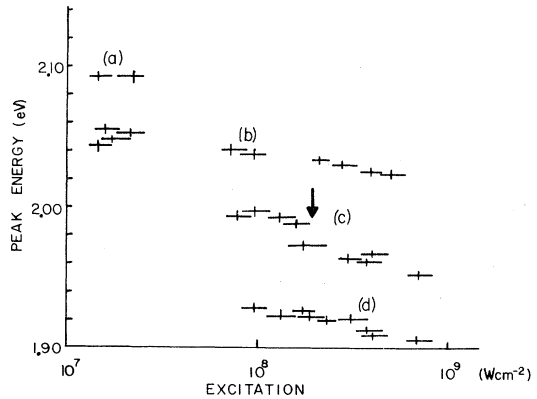

FIG. 5. Peak energies of the higher- and lower-energy bands at 77 and 300 K as functions of the excitation intensity. (a) Higher-energy band at 77 K. (b) Lower-energy band at 77 K. (c) Higher-energy band at 300 K. (d) Lower-energy band at 300 K.

as a function of excitation intensity. The error bars of the peak energies were determined from the spectral resolution of the measuring system. In Fig. 5(a), the peak energy of the higher-energy band at 77 K, is close to a constant within experimental error between the excitation intensities of 1.3×10^7 to 2.5×10^7 W cm^{-2}; in 5(b), the peak energy of the lower-energy band at 77 K decreases continuously from 1.3×10^7 to 6×10^8 W cm^{-2}; in 5(c), the peak energy of the higher-energy band at 300 K is close to a constant (~1.994 eV) within experimental error below the excitation 1.6×10^8 W cm^{-2} and starts to decrease above the excitation 1.7×10^8 W cm^{-2}; and in 5(d), the peak energy of the lower-energy band at 300 K decreases continuously from 8×10^7 to 8×10^8 W cm^{-2}.

IV. DISCUSSION

A. Higher-energy band

In the preceding section we presented data on the time-integrated photoluminescence at different excitation intensities. In this section the shape of the high-energy tail of the higher-energy luminescence band will be analyzed using the theoretical expressions for exciton-electron (-hole) scattering emission, exciton-exciton scattering emission, and electron-hole plasma emission processes in the different intensity regions.

The theoretical expression for the luminescence shape arising from exciton-electron (-hole) scattering emission is given by[12]

$$P_s(h\nu)\propto\frac{1}{\beta_e}\frac{N_0\eta_0}{(E_0-h\nu)^2+(\pi\gamma/\epsilon)E_0^2}\times\left[\frac{\alpha_2}{\alpha_1}\right]^{1/2}K_1[2(\alpha_1\alpha_2)^{1/2}]\times\exp\left[\frac{m_{h(e)}}{2M}(E_0-h\nu)\right],\tag{1}$$

where

$$\alpha_1\equiv\frac{\hbar^2\beta_e}{2M}\left|\frac{\beta_L}{\beta_e}+\frac{M_{h(e)}^2}{4M_{e(h)}M}\right|,$$

$$\alpha_2\equiv\frac{M_{e(h)}\beta_e}{2\hbar^2}(E_0-h\nu)^2,$$

E_0 is the exciton energy, $\beta_e\equiv1/kT_e$, and $\beta_L\equiv1/kT_L$. The above symbols are defined as follows: T_e and T_L are the temperatures of carriers and lattice, respectively; N_0 and η_0 are the occupation number of excitons and electrons (holes) for a null wave vector, respectively; $K_1(x)$ is the first-order modified Bessel function of the third kind; $M=m_e+m_h$ is the effective mass of the exciton; $\pi\gamma/\epsilon$ is the exciton-photon coupling, which is not known for GaSe. We choose $\pi\gamma/\epsilon\sim2.5\times10^{-4}$ from CdS as a typical value, and $m_e=0.2m_0$, $m_h=0.5m_0$.[13]

The theoretical expression for the luminescence shape arising from exciton-exciton scattering emission is as follows[14]:

$$P_s(h\nu)\propto\frac{h\nu P(h\nu)}{(E_0-h\nu)^2+(\pi\gamma/\epsilon)E_0^2}\frac{N_0^2}{kT_L}\int_0^\infty d\xi\int_0^\infty dt\frac{\xi^{1/2}}{(1+\xi/E_x^b)^4}\exp\left[-t-\frac{1}{4t}\left[\frac{E_0-E_x^b-h\nu-\xi}{kT_L}\right]^2\right],\tag{2}$$

where $\rho(h\nu)d\nu$ is the number of photon modes in the crystal between the frequencies ν and $\nu+d\nu$, and E_x^b is the binding energy of the exciton.

The theoretical expression for the shape of luminescence arising from electron-hole plasma emission with K selection at high temperature is given by[15]

$$P_s(h\nu)\propto(h\nu-\tilde{E}_g)^{1/2}\exp[-(h\nu-\tilde{E}_g)/kT_e]\tag{3}$$

where $\tilde{E}_g+\frac{1}{2}kT_e$ is equal to the peak energy of the emission band.

At 77 K the high-energy side of the higher-energy band can be fitted by the exciton-electron (-hole) scattering process given by Eq. (1) with $T_e=T_L=77$ K, $E_0=2.098$ eV for Fig. 1(a) and 1(b). In Fig. 6 the dots with error bars are the experimental data while the solid line is the theoretical fits by Eq. (1). As the excitation increases, the higher-energy band of Fig. 1(c) is very small in intensity relative to the lower-energy band. At 2.5×10^7 W cm^{-2}, the higher-energy band does not grow as fast as the lower-energy band as shown in Figs. 1(d) and 1(e).

At room temperature, the higher-energy bands from Figs. 2(a)–2(d) can also be fitted by Eq. (1) on the high-energy tails with $T_e=T_L=300$ K and

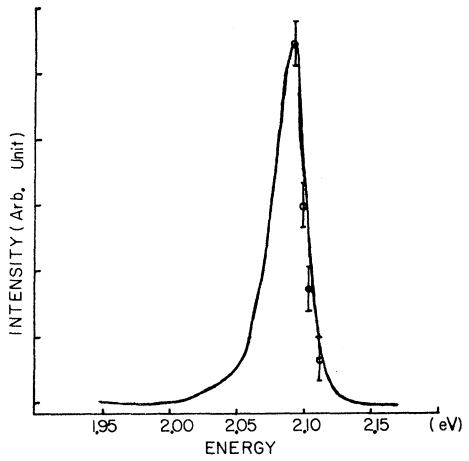

FIG. 6. High-energy tail of the higher-energy band at 77 K of Fig. 1(a) is fitted by the theoretical expression of exciton-electron (-hole) scattering emission. The dots with error bar means the experimental results. The solid line represents the theoretical fit by Eq. (1).

$E_0=2.0$ eV. This is shown in Fig. 7. These curves are for excitation intensities less than 1.7×10^8 W cm^{-2}. For higher-excitation intensities, the high-energy tails of the higher-energy bands can no longer be fitted by Eq. (1) with $T_e=T_L=300$ K and $E_0=2.0$ eV. The high-energy tail of the higher-energy band of Fig. 2(e) can be fitted by Eq. (1) using $T_e=2000$ K, $T_L=300$ K, and $E_0=1.979$ eV. But higher carrier temperature and smaller exciton energy are unreasonable because the carrier temperature should not change from 300 to 2000 K when the excitation changes from 1.61×10^8 W cm^{-2} of Fig. 2(d) to 1.70×10^8 W cm^{-2} of Fig. 2(e). Also the exciton energy should not change at different excitation intensities. It has been shown by picosecond absorption spectroscopy[16] on GaSe that the hot photogenerated carriers thermalize within 100 ps to the lattice temperature. Since the photoluminescence recombination time[16] ($\sim$300 ps) is much longer than 100 ps, the time-integrated emission will be from excitations thermalized with the lattice.

The peak energy of the theoretical formula for the exciton-exciton scattering would be at 2.078 eV (2.0 eV), with $E_0=2.098$ eV (2.0 eV), and $E_x^b=20$ meV, when the sample is at 77 K (300 K). As shown in Figs. 8 and 9, the theoretical expressions for the exciton-exciton scattering emissions at 77 and 300 K are represented by solid lines and the experimental data from Figs. 1(a) and 2(c) are represented by dots with error bars. It is clear that Eq. (2) cannot fit the high-energy tails of the higher-energy bands of the photoluminescence spectra for both temperatures.

As shown in Fig. 5(c), the peak energies of higher-energy bands shown in Figs. 2(a)–2(d) for excitation intensities smaller than 1.7×10^8 W cm^{-2} are almost the same value ($\sim$1.994 eV). There is a sudden decrease by $\sim$20 meV for the peak energy shown in Fig. 2(e) when the excitation is $\sim1.7\times10^8$ W cm^{-2}. For larger excitation intensities, the peak energy decreases monotonically shown in Figs. 2(e)–2(h). It is reasonable to guess that the emission is from the electron-hole plasma in this latter region given by Eq. (3). Using Eq. (3), the high-energy tails of the higher-energy bands displayed

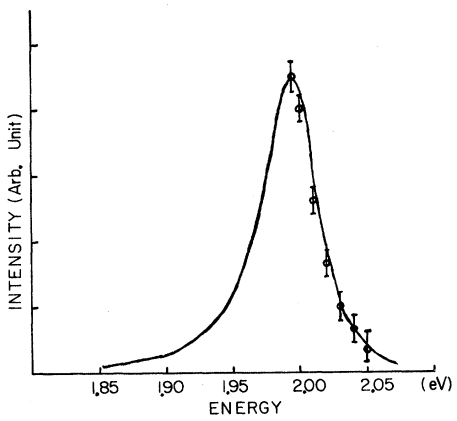

FIG. 7. High-energy tail of the higher-energy band at 300 K of Fig. 2(a) is fitted by the theoretical expression of exciton-electron (-hole) scattering emission. The dots with error bars means the experimental result. The solid line means the theoretical fit by Eq. (1).

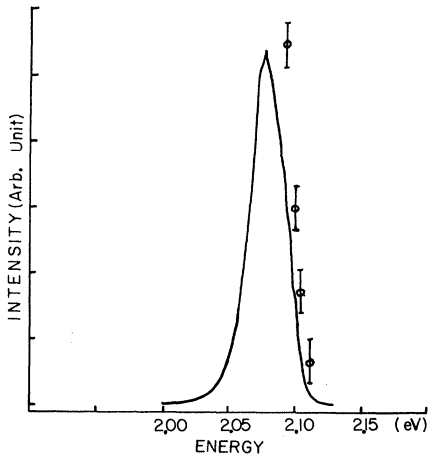

FIG. 8. High-energy tail of the higher-energy band of Fig. 1(a) is not fitted by Eq. (2).

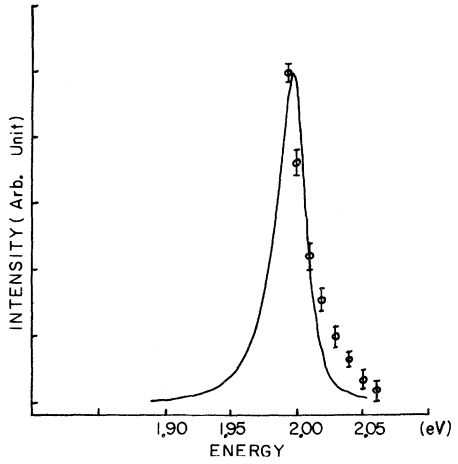

FIG. 9. High-energy tail of the higher-energy band of Fig. 2(c) is not fitted by Eq. (2).

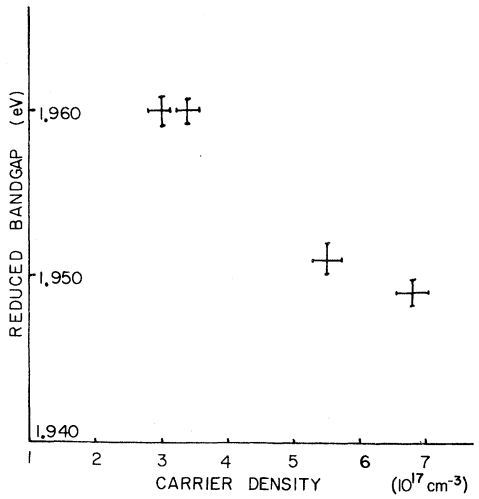

FIG. 11. Reduced band gap from the higher-energy band of the emission spectra as a function of the carrier density at room temperature.

from Figs. 2(e) to 2(h) can be fitted with $T_e = 300$ K as shown in Fig. 10. The solid line is from Eq. (3) and the dots with error bars are the experimental data from Fig. 2(e). The value of $\tilde{E}_g$ as a function of the carrier density is plotted in Fig. 11. The carrier density was calculated using the measured absorption coefficient, values of incident light energy, and loss of scattered light. For the excitation intensity $(1.70\pm0.25)\times10^8$ W cm^{-2} of Fig. 2(e), the calculated density is 3×10^{17} cm^{-3}. The absorption constant[17] at 530 nm is 2×10^3 cm^{-1}. In this sample, 97% of incident light is not absorbed due to scattering of incident light as determined from the absorption measurement.[16] As shown in Fig. 11, the reduced band gap becomes smaller when the carrier density increases.

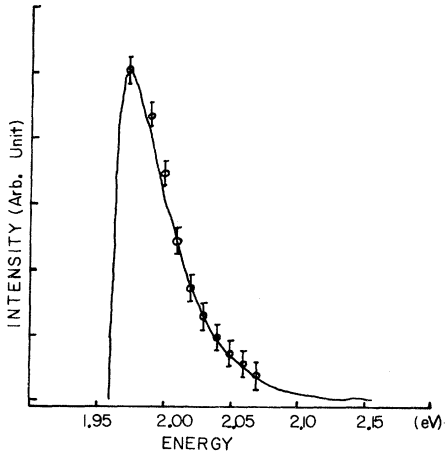

FIG. 10. High-energy tail of the higher-energy band at 300 K of Fig. 2(f) is fitted by an expression of plasma emission of Eq. (3) with K selection. The dots with error bar means the experimental result. The solid line is the theoretical fit.

From the analysis of the high-energy tails and the peak energies of the higher-energy bands, we found that at room temperature the exciton-electron (-hole) scattering emission disappears when the excitation intensity reaches $(1.70\pm0.25)\times10^8$ W cm^{-2} as shown in Figs. 2(e) and 5. Above this intensity the electron-hole plasma emission appears.

From the data displayed in Fig. 4(a), the emission intensity is linearly proportional to the excitation intensity for both the exciton-electron (-hole) scattering emission and the plasma-emission regions. Since the exciton-electron (-hole) scattering is proportional to the numbers of excitons and electrons (holes) as shown in Eq. (1), and the plasma emission is proportional to the numbers of electrons and holes. The numbers of excitons, electrons, and holes are all linearly proportional to the square root of excitation intensity[12] at high excitations; therefore, the intensity dependences of both exciton-electron (-hole) scattering emission and the plasma emission are linear with the excitation intensity.

Although the direct exciton binding energy is 20 meV,[18] the exciton-electron (-hole) scattering emission can still be observed at room temperature because of the existence of the excitons.[19] Comparing the data in Figs. 3(b) and 4(b), we observed that the threshold for the stimulated emission occurs at a much higher excitation intensity ($\sim3\times10^8$ W cm^{-2}) than that at 77 K ($\sim10^7$

$W\,cm^{-2}$). Therefore, this gave us a wider intensity region at room temperature to observe the change from exciton-electron (-hole) scattering emission to electron-hole plasma emission.

B. Lower-energy band

From the data displayed in Figs. 3(b) and 4(b), we can conclude that the lower-energy bands at both temperatures arise from stimulated emission. The peak energies of the lower-energy bands are located about 50 meV or more below the higher-energy bands. Many processes have been proposed earlier to account for this stimulated emission: the exciton-carrier complex,[20] the exciton-exciton scattering,[7] the exciton-electron scattering,[8] and the Auger process due to the direct and indirect excitons.[9] At room temperature, the excitation intensity required for stimulated emission is larger than $1.7\times10^{8}\ W\,cm^{-2}$. Since the exciton-carrier scattering emission disappears above this intensity, a possible mechanism for the stimulated emission process involves only free carriers of plasma from the indirect gap. Since the knowledge of the electronic energy-band diagram of GaSe is not complete at this time, it is difficult to determine the exact mechanism for the stimulated emission process.

V. CONCLUSION

We have observed two emission bands at 77 and 300 K. The higher-energy band is the exciton-electron (-hole) scattering emission at lower excitation intensity and the electron-hole plasma emission at higher excitation intensity. The transition was observed from the exciton carrier scattering emission to the electron-hole plasma emission in GaSe under high-power picosecond laser excitations at room temperature. We also found the reduced band gaps in some region of high carrier density. The lower-energy bands are stimulated emissions. The threshold for the stimulated emission is lower at 77 K than at 300 K.

ACKNOWLEDGMENTS

We thank the U. S. Air Force Office of Scientific Research Grant No. 80-0079 for the support of this research. We also thank Dr. J. Buchert for his help in computer programming.

[1]Ph. Schmid and J. P. Voitchovsky, Phys. Status Solidi B 65, 249 (1974).
[2]M. Schlueter, Nuovo Cimento B 13, 311 (1973).
[3]Y. Sasaki and Y. Nishina, Phys. Rev. B 23, 4089 (1981).
[4]A. Mercier, E. Mooser, and J. P. Voitchovsky, Phys. Rev. B 12, 4307 (1975).
[5]R. E. Nahory, K. L. Shaklee, R. F. Leheny, and J. C. DeWinter, Solid State Commun. 9, 1107 (1971).
[6]T. Ugumori, K. Masuda and S. Namba, Solid State Commun. 12, 389 (1973).
[7]T. Ugumori, K. Masuda, and S. Namba, J. Phys. Soc. Jpn. 41, 1991 (1976).
[8]A. Mercier and J. P. Voitchovsky, Phys. Rev. B 11, 2243 (1975).
[9]N. Kuroda and Y. Nishina, J. Lumin. 12/13, 623 (1976).
[10]R. Baltramiejunas, V. Narkevicius, E. Skaistys, J. Vaitkus, and J. Viscakas, Nuovo Cimento B 38, 603 (1977).
[11]A. Cingolani, M. Ferrara, and M. Lugara, Opt. Commun. 32, 109 (1980).
[12]C. Benoit a La Guillaume, J. M. Debever, and F. Salvan, Phys. Rev. B 177, 567 (1969).
[13]G. Ottaviani, C. Canali, F. Nova, Ph. Schmid, E. Mooser, R. Minder, and I. Zschokke, Solid State Commun. 14, 933 (1974).
[14]T. Moriya and T. Kushida, J. Phys. Soc. Jpn. 40, 1668 (1976).
[15]Y. Yoshikuni, H. Saito, and S. Shionoya, Solid State Commun. 32, 665 (1979).
[16]S. S. Yao, J. Buchert, and R. R. Alfano, Phys. Rev. B 25, 6534 (1982).
[17]G. Antonioli, D. Bianchi, V. Emiliani, P. Podini, and P. Franzosi, Nuovo Cimento B 54, 211 (1979).
[18]J. L. Staehli and A. Frova, Physica (Utrecht) 99B, 299 (1980).
[19]J. P. Voitchovsky and A. Mercier, Nuovo Cimento B 22, 273 (1974).
[20]R. C. C. Leite, E. A. Mineses, N. Jannuzzi, and J. G. P. Ramos, Solid State Commun. 11, 1741 (1972).